Proceedings of IMECE2009
2009 ASME International Mechanical Engineering Congress and Exposition
November 13-19, Lake Buena Vista, Florida, USA

DRAFT **IMECE2009-12634**

SIMULATION OF COMBUSTION AND THERMAL-FLOW INSIDE A PETROLEUM COKE ROTARY CALCINING KILN, PART 1: PROCESS REVIEW AND MODELING

Zexuan Zhang
Research Assistant
Zzhang@uno.edu

Ting Wang
Professor
Twang@uno.edu

Energy Conversion and Conservation Center
University of New Orleans
New Orleans, LA 70148-2220, USA

ABSTRACT

Calcined coke is an important material for making carbon anodes for smelting of alumina to aluminum. Calcining is an energy intensive industry and a significant amount of heat is wasted in the calcining process. Efficiently managing this energy resource is tied to the profit margin and survivability of a calcining plant. To help improve the energy efficiency of the calcining process, a 3-D computational model is developed to gain insight of the thermal-flow and combustion behavior in the calciner. Comprehensive models are employed to simulate the moving petocke bed with moisture evaporation, devolatilization, and coke fines combustion with a conjugate radiation-convection-conduction calculation.

NOMENCLATURE

a	Local speed of sound (m/s)
c	Concentration (mass/volume, moles/volume)
c_p, c_v	Specific heat at constant pressure, volume (J/kg-K)
D_{ij}	Mass diffusion coefficient (m^2/s)
E	Total energy, activation energy (J)
f	Mixture fraction (dimensionless)
g	Gravitational acceleration (m/s^2)
H	Total enthalpy (energy/mass, energy/mole)
h	Heat transfer coefficient (W/m^2-K)
h	Species enthalpy (energy/mass, energy/mole)
h_0	Standard state enthalpy of formation (energy/mass, energy/mole)
I	Radiation intensity (energy per area of emitting surface per unit solid angle)
J	Mass flux; diffusion flux (kg/m^2-s)
K	Equilibrium constant = forward rate constant / backward rate constant (units vary)
k	Kinetic energy per unit mass (J/kg)
k	Reaction rate constant, e.g., k1, k-1, $k_{f;r}$, $k_{b;r}$ (units vary)
k	Thermal conductivity (W/m-K)
k_B	Boltzmann constant (1.38×10^{-23} J/mole-K)
k, k_c	Mass transfer coefficient (units vary)
l, L	Length scale (m, cm)
m	Mass (kg)
$\dot{m}$	Mass flow rate (kg/s, kg/hr, metric ton/hr)
M_w	Molecular weight (kg/kgmol)
M	Mach number
Nu	Nusselt number ≡ hL/k (dimensionless)
p	Pressure (Pa, atm)
Pr	Prandtl number = α/ν (dimensionless)
Q	Flow rate of enthalpy (W)
q"	Heat flux (W/m^2)
R	Gas-law constant (8.31447×10^3 J/kgmol-K)
r	Radius (m)
R	Reaction rate (units vary)
Re	Reynolds number ≡ UL/ν (dimensionless)
S	Total entropy (J/K)
s	Specific entropy(J/K-kg)
s_0	Standard state entropy (J/K)
Sc	Schmidt number = ν/D (dimensionless)
S_{ij}	Mean rate-of-strain tensor (s^{-1})
T	Temperature (K, °C)
t	Time (s)
t	Thickness (m)
u, v, w	Velocity components (m/s); also written with directional sub-scripts (e.g., v_x, v_y, v_z, v_r)
U	Free-stream velocity (m/s)
V	Volume (m^3)
V	Volume flow rate (SCFM)
$\vec{v}$	Overall velocity vector (m/s)
X	Mole fraction (dimensionless)
Y	Mass fraction (dimensionless)

Greek Letters

α	Permeability, or flux per unit pressure difference (L/m^2-hr-atm)
α	Volume fraction (dimensionless)
α	Thermal diffusivity (m^2/s)
β	Coefficient of thermal expansion (K^{-1})
γ	Specific heat ratio, c_p/c_v (dimensionless)
δ	Delta function
Δ	Change in variables)
ε	Emissivity (dimensionless)
ε	Turbulent dissipation rate (m^2/s^3)
η′,η″	Rate exponents for reactants, products (dimensionless)
θ_r	Radiation temperature (K)
ν	Kinematic viscosity (m^2/s)

μ	Dynamic viscosity (Pa-s)
ν',ν''	Stoichiometric coefficients for reactants, products
ρ	Density (kg/m^3)
σ	Stefan-Boltzmann constant (5.67×10^{-8} W/m^2-K^4)
σ_s	Scattering coefficient (m^{-1})
$\bar{\bar{\tau}}$	Stress tensor (Pa)
τ	Shear stress (Pa)
τ	Time scale, e.g., τ_c, τ_p (s)
Φ	Equivalence ratio (dimensionless)
Φ	Diameter (m)

INTRODUCTION

Background

Petroleum coke (or petcoke) is a carbonaceous solid derived from petroleum refinery cracking process. Calcination is the process of heating a substance to a high temperature, but below its melting or fusing point, to bring about thermal decomposition or a phase transition in its physical or chemical constitution. Petroleum coke is usually calcined in a gas-fired rotary kiln or rotary hearth at high temperatures, around 1,200 to 1,350 °C, to remove moisture, drive off volatile matters, increase the density of the coke structure, increase physical strength, and increase the electrical conductivity of the material (Fig.1). The product is hard, dense carbon (calcined petroleum coke) with low hydrogen content and good electrical conductivity. These properties along with the low metals and ash contents make calcined petroleum coke the best material currently available for making carbon anodes for smelting of alumina to aluminum [1]. In addition, calcined coke is used in many other industries such as the manufacturing of graphite electrodes, titanium dioxide, and steel (to increase the carbon levels). The largest consumer of the calcined coke is the aluminum industry, at more than 70 % of the world's total.

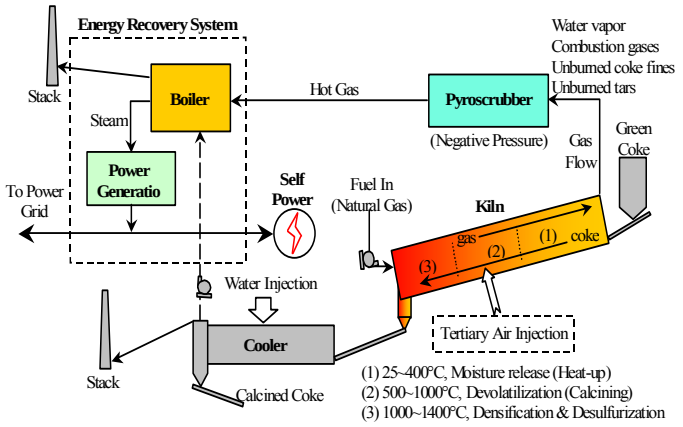

Fig. 1 Schematic of calcining process for petroleum coke

Calcination is an energy intensive process. During the petroleum coke calcination, energy input is needed to heat up the petroleum coke and maintain the required calcining kiln temperature to produce the desired calcined petroleum coke quality. Meanwhile, volatile matters, producer gas, and a significant amount of waste heat are generated from the calcining process. Efficiently managing these energy resources is necessary for increasing the profit margin and survivability of a calcining plant.

Currently, natural gas is used for the kiln's primary combustion. In fact, the calcining process produces more energy from the volatiles in the petroleum coke than the theoretical energy needed for the calcining process. The ideal system would, except for start up, not need to burn natural gas because the energy from the petroleum coke could be utilized instead. In view of the continuously rising natural gas price, minimizing natural gas consumption is essential to reducing production cost as well as avoiding unsteady impact on profit margin exerted by fluctuating natural gas price.

To minimize or remove natural gas consumption, a thorough 3-D modeling and analysis of the calcining process in the kiln are essential. The detailed dynamic simulation in the kiln will gain insights into the thermal-flow and chemical reaction process in the kiln, including 3-D flow pattern, the turbulence structure, the combustion process, the local heat release rate, heat transfer process, temperature distribution, and species concentration distributions. With the established detailed simulation, various means can be quickly simulated by the computer to effectively use the producer gases (volatile matters, CO and H_2), control the combustion rate, and manipulate heat distribution. This study employs the Computational Fluid Dynamics (CFD) simulation to show what happens at any location inside the kiln and help engineers make decisions on how to utilize the volatiles derived from the petroleum coke, and ultimately, eliminate the use of natural gas.

Fluid velocity, pressure, temperature, and chemical reactions can be analyzed by using CFD scheme and appropriate models throughout the computational domain with complicated geometries and boundary conditions. During the analysis, modifications of geometries or boundary conditions can be easily applied to view their impact on the thermal flow patterns or species concentration distributions. This study will investigate the potential means to reduce energy cost of the calcining process using a rotary kiln.

Objectives

To reach the ultimate goal of cutting the energy costs of the calcining process, it is necessary to understand in greater detail the thermal-flow and combustion process inside the kiln. To this end, the objective of this study is to model and simulate the thermal-flow and combustion behavior of an industry petroleum coke calcining rotary kiln. The specific goals are

1. To develop a numerical model to simulate the combustion, gas phase and solid phase motion in the kiln;
2. To investigate the flow pattern, combustion, and temperature distribution inside the kiln;
3. To study the effect of different tertiary air injection angle;
4. To study the moving bed and conjugate heat transfer situation;
5. To identify the means that can help reduce natural gas consumption and increase kiln energy efficiency.

Limited to the paper length, Part 1 of this paper presents goal 1. Part 2 will present goals 2 and 3. The results of goals 4 and 5 will be presented in a future paper.

LITERATURE SEARCH

Calcination

For continuous calcinations of petroleum coke (petcoke), the **rotary kiln** and the **rotary hearth** furnace are the two primary methods commonly used in the calcining industry all over the world [2].

Introduction of Rotary Kiln

Kiln: Most petroleum coke is calcined in a rotary kiln. A rotary kiln is a slightly tilted horizontal cylinder rotating at a controlled slow rate. An industrial rotary kiln is typically of 2.5 to 5 meters in diameter, 50 to 80 meters in length, and insulated with 0.23 meter thick high-temperature refractory bricks inside the kiln. The

kiln shell is made of 25 mm thick steel with sections under the kiln tires being 50 to 70 mm thick. The kiln shell is supported by tires, which ride on two wheels or trunions. The kiln is rotated via a large bull gear that is larger than the diameter of the kiln shell and is driven by one or two spur gears. The spur gears are driven through a gearbox by either a direct electrical drive or by hydraulic motors.

Calcining Process Flow: Raw petroleum coke is sized to 50 to 100 mm lump and fed to raw feed silos, then to the feed end of the rotary kiln (at the high end) through a side feed scoop or through a feed pipe (in older units). The kiln is sloped downward towards the discharge end at a slope of 4.16 to 6.23 cm per meter. After entering the rotary kiln, moisture is driven off the petroleum coke in the "Heat-up Zone." Devolatilization occurs mostly at 500°C to 1,000°C in the "Calcining Zone". Further dehydrogenation and some desulfurization take place in the "Calcined Coke Zone" at 1,200°C to 1,400°C. In this zone, the petroleum coke structure densifies and shrinks. As the petroleum coke progresses down the rotary kiln countercurrent to the hot combustion gases, the temperature increases to a maximum temperature of around 13 to 20 meters before the discharge end of the rotary kiln. The petroleum coke moves through the rotary kiln in about 40 to 60 minutes. It then drops off at the discharge end of the rotary kiln through a refractory-lined chute and into a rotary cooler.

Cooler: The cooler is a bare steel cylinder similar to the rotary kiln, but it is usually smaller in diameter, shorter, and rotated at higher rpm's than a rotary kiln with water sprays in the front end. Water is sprayed and in contact with the hot calcined petroleum coke, using the latent heat of vaporization of the water for cooling. In places where water quality is poor and not suitable for direct cooling, indirect water-cooled rotary cylinder coolers are used. The calcined petroleum coke stays about 20 minutes in the cooler and is then discharged onto high temperature conveyor belts or into screw feeders. Computer controls and adjusts the water sprays to maintain the temperature of the calcined petroleum coke at around 120°C to 180°C at the cooler exit, to keep the calcined product dry.

Firing Crown and Heat Transfer: At the discharge end of the rotary kiln, a burner is installed in the firing crown (a hood that fits over the discharge end of the rotary kiln) to preheat the refractory before startup and to supply heat for maintaining the coke bed at certain temperatures in most applications. Most kiln burners are natural gas fired, but some older model kilns have oil-fired burners. Primary combustion air is also injected through the firing crown. Some kilns use oxygen instead of air to reduce emissions, especially the thermal NO_x. The temperature of the discharging calcined petroleum coke is monitored by an optical pyrometer. The temperature is controlled by the amount of natural gas, excess combustion air, rotary kiln rotation speed, and raw petroleum coke feed rate. As illustrated in Fig. 2, almost all of the heat transfer to the coke bed is by radiation and convection from the gases inside the rotary kiln and exposed portions of the refractory wall. A recent transient analysis by Zhao and Wang [3] showed that only a small amount of heat is transferred by conduction from the refractory brick layer to the material. Analysis of either the real density or the electrical resistivity of the calcined coke measures the degree and quality of calcination process.

Tertiary Air Injection: Since the volatiles coming off the coke during calcination contain approximately 1.5 to 2 times of the fuel value (1,343 kJ/kg) required for the calcining process, these volatile matters are ideal to be utilized for the calcining process. Tertiary air is injected into the calcining zone through the side of the kiln from shell mounted blowers to burn the volatile matters and forms a second hot zone extending upward to the feed end of the kiln (Fig. 3). Many rotary kilns use tertiary air to combust petcoke dust and volatiles for the advantage of increasing production rates and decreasing the natural gas consumption. The major disadvantage of using tertiary air is a faster up-heat rate in the critical range of 500 to 700 °C [4] may result in poorer coke quality than without tertiary air.

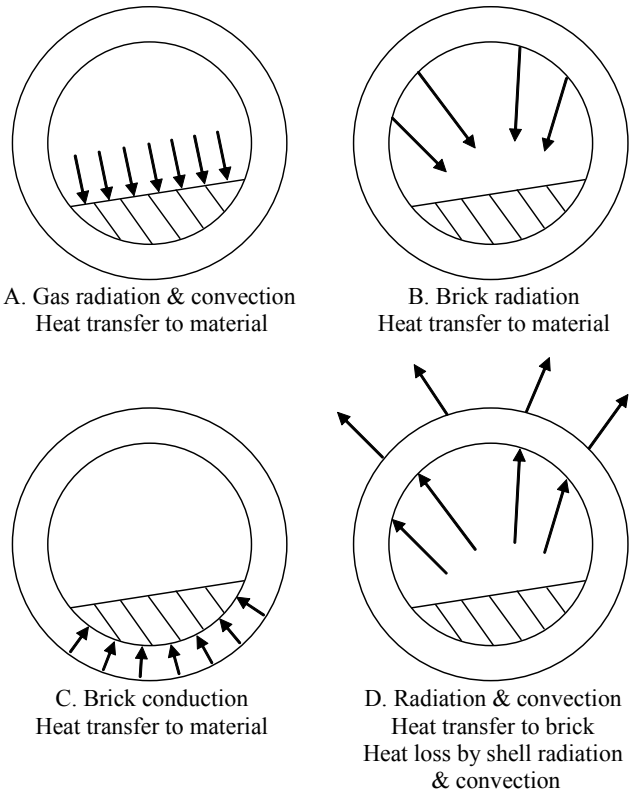

Fig. 2 Heat transfer mechanism in a rotary kiln [1]

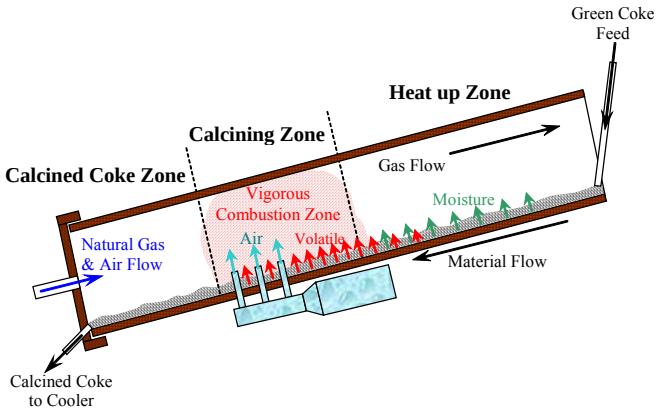

Fig. 3 Petroleum coke calcination with tertiary air

Rotary Kiln Operation: Some of the key control parameters for operating a rotary kiln and producing good quality calcined coke include sizing of the petcoke, the control of the up-heat rate of the raw petcoke, and the feed consistency of raw petcoke. Slow up-heat rate is critical to the calcining process. The typical good practice of calcining petcoke for the aluminum industry is to slowly heat the pecoke around 500 to 600 °C during the initial devolatilization, so the mesophase or liquid crystal part of the petcoke does not bloat or distort (like pop-corn) during the devolatilization process. Petcoke with anisotropic (needle) structure and high volatile matters must be calcined with slow up-heat rates to produce good calcined densities and low porosity.

Some attempts have been made to stir the coke bed using "tumblers," also called "lifters," in kilns to increase production and

keep the coke up-heat rate down [5]. Tumblers are castable refractory or refractory bricks that stand above the surrounding bricks. The use of a tumbler has successfully resulted in increased production; however, the optimum location for installing a tumbler is not yet known. There is a problem with keeping tumblers in a rotary kiln. Refractory bricks and the steel shell of a rotary kiln both expand. Bricks must expand enough as not to be too loose in the kiln to prevent excess migrating, yet not so tight, as to exceed the hot crushing strength of the brick. Tumblers get hotter at their tips, have a pinch point at the interface of the surrounding bricks, and are subject to breaking at the interface. Several complete rings of taller bricks seem to hold together, but the adjacent bricks on the upside (the side facing the rotating direction) wear out earlier due to a stagnant layer of coke that grinds down the bricks. Tumblers can also cause the other problem when a coke bed is stirred too much: The coke fines are entrained into combustion gases and reduce the calcined coke production rate.

The degree of petroleum coke calcination depends mostly on variations in the raw petcoke such as differences in structure, volatile matters, and particle sizing. In rotary kilns, it has been documented that coarse particles travel faster through the rotary kiln than the finer particles. Some calciners have stated that coarser coke with lower quantities of fines can increase the production rate in a rotary kiln. Without proper sizing and feeding of a rotary kiln, slides can occur and will dump most of the incomplete product rapidly out of the rotary kiln. Rapid devolatilization in the calcining zone tends to fluidize the petcoke. Excessive fluidization causes the slides.

Introduction of Rotary Hearth

The other commercial method of calcining petcoke employs rotary hearth calciners. Marathon Oil and Wise Coal and Coke Company jointly developed the rotating hearth furnace for calcining coal and adapted the technology for calcining petcoke [6]. The first rotary hearth petcoke calciners were located in Europe.

The rotary hearth consists of a large rotating disk-type furnace that slopes from the outside toward the center. Raw coke is fed into the outer edge of the rotary hearth and is plowed inward with water-cooled plows called rabbles that push the coke toward the center. The rabbles can be adjusted to control the coke bed depth leaving enough stagnant coke to prevent wear of the refractory. Coke fines usually deposit onto the coke bed thus eliminating any entrainment with the combustion gases above the coke bed. The stirring of the coke bed is critical for good heat transfer so that all coke can reach calcinations temperature. After passing through a center-soaking pit, the hot coke falls through a rotating discharge table into a cooler.

Burners and combustion air nozzles are located on a stationary, suspended roof that is connected to the rotating hearth with a seal between the two. After start-up, the rotary hearth calciner makes use of the complete combustion of the volatile matters of the raw coke feed. Little or no excess fuel is required for heating. The hot combustion gases coming off the top center of the roof are used to preheat the combustion air in some hearths to further improve combustion efficiencies. The small amount of coke fines and the volatile matters from the coke are completely consumed in the roof of the hearth, so no external incinerator is required.

Combustion

Combustion or burning is a complicated sequence of chemical reactions between a fuel and an oxidant accompanied by the production of heat or both heat and light in the form of either a glow or flames. In a complete combustion reaction, a compound reacts with an oxidizing element at the maximum percentage, and the products are compounds of each element in the fuel with the oxidizing element. The complete global combustion reaction of carbon with oxygen is:

$$C + O_2 \rightarrow CO_2 + \text{Heat} \quad \text{(Eq.1)}$$

In reality, combustion processes are never perfect or complete. In flue gases from combustion of carbon (Eq.2) or carbon compounds (as in combustion of hydrocarbons, wood etc.) both unburned carbon (known as soot) and carbon compounds (CO in Eq.3) and others) will be present.

$$C + \tfrac{1}{2}O_2 \rightarrow CO + \text{Heat} \quad \text{(Eq.2)}$$

$$CO + \tfrac{1}{2}O_2 \rightarrow CO_2 + \text{Heat} \quad \text{(Eq.3)}$$

Also, when air is the oxidant, some nitrogen will be oxidized to various, mostly harmful, nitrogen oxides (NO_x). The effectiveness of combustion can be determined by analyzing the flue gas and the amount of soot.

There are three types of fuel present in the calcining process, methane (as natural gas), carbon (as petcoke), and volatile matters (as hydrocarbons).

The complete global combustion of methane and volatile matters can be presented as:

$$CH_4 + 2O_2 \rightarrow CO_2 + 2H_2O + \text{Heat} \quad \text{(Eq.4)}$$

$$C_xH_yO_z + \left(x + \tfrac{y}{4} - \tfrac{z}{2}\right)O_2 \rightarrow xCO_2 + \tfrac{y}{2}H_2O + \text{Heat} \quad \text{(Eq.5)}$$

Calcined Petroleum Coke Properties

The calcined petroleum coke properties need to meet the specifications for anode grade coke for aluminum smelting industries. The physical properties include real density, electrical resistivity, Hg apparent density, vibrated bulk density, hardgrove grindability index, pulverization factor, grain stability, crystallite thickness, interlayer spacing, shot coke content, screen sizing, air and CO_2 reactivities. The chemical properties include volatile matters, hydrogen, moisture, ash, sulfur, metals, and nitrogen.

PROBLEM SETUP AND MODELING

The overall design of the studied rotary calcining kiln is shown in Fig. 4. The model is developed and meshed using GAMBIT. The studied domain basically consists of three sections: the calcined coke zone (Fig. 5), the calcining zone (Fig. 6), and the heat-up zone (Fig. 7). The fresh green petcoke is fed from the entrance of the heat-up zone (right upper end in Fig. 4) and discharged at the end of the calcined coke zone (left lower end in Fig. 4). The primary injection of air and fuel (natural gas) is located at the firing crown at the end of the calcined coke zone. In the calcining zone, six tertiary injectors are aligned along the kiln wall in a form of two longitudinal arrays located diametrically opposite to each other as shown in Figs. 6 and 8. The downstream tertiary injectors are labeled as D1, D2, and D3, while the upstream injectors are labeled as U1, U2, and U3. Those injectors provide the necessary air to combust the volatile matters in the calcining and heat-up zones. The fuel used in the primary injection is methane, CH_4. It is burned in the calcined coke zone to control the temperature and hence the quality of the calcined coke product.

The problem is modeled with the following general assumptions:

1. Three dimensional, steady and incompressible flow
2. Constant material properties for the coke bed
3. Variable material properties for air and reacted gases
4. Buoyancy force neglected
5. No-slip condition (zero velocity) on wall surfaces
6. Turbulent flow
7. Chemical reactions are faster than the time scale of the turbulence eddies, so the reaction rates are controlled by the turbulence eddy size and dynamics.

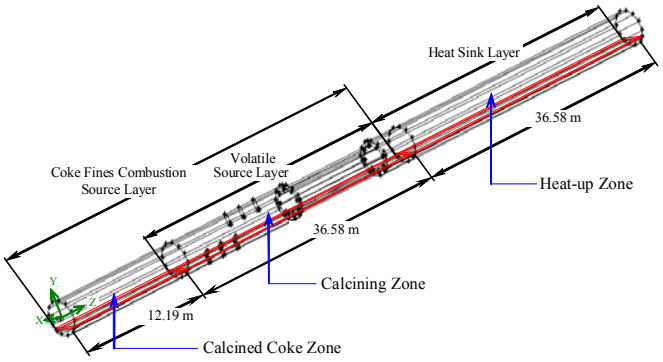

Fig. 4 A 3-D view of the simulated calcining rotary kiln

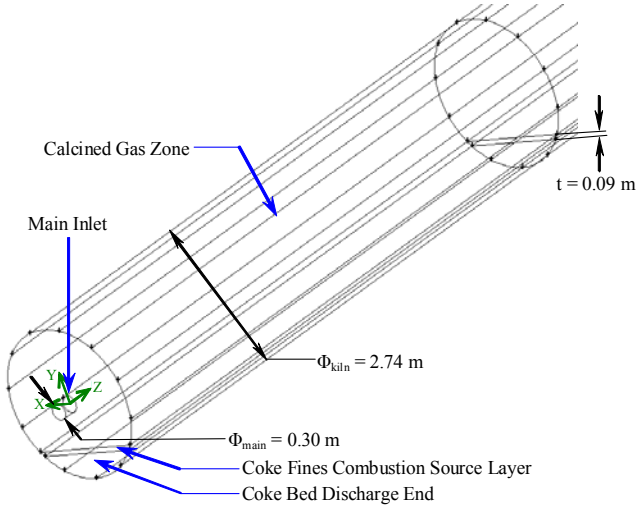

Fig. 5 Detailed view of calcined coke zone near the discharge end

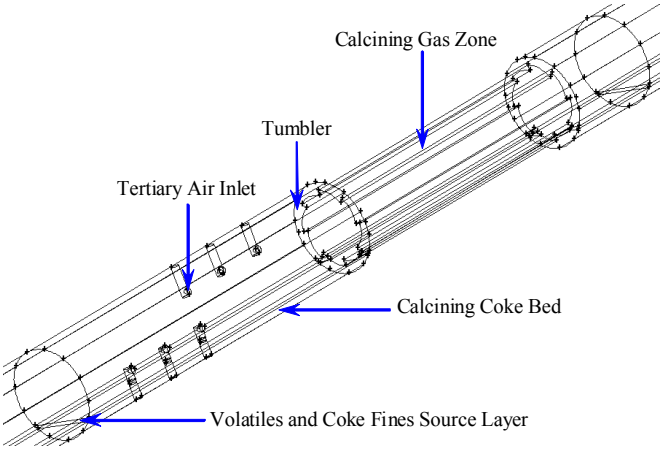

Fig. 6 Detailed view of calcining coke zone including tertiary air injectors and tumblers

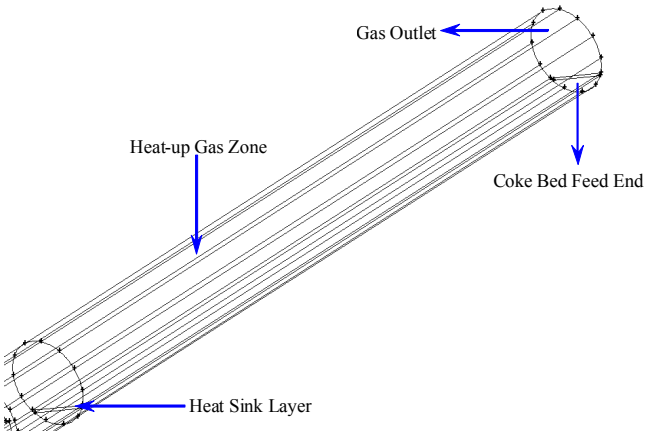

Fig. 7 Close-up view of the heat-up zone

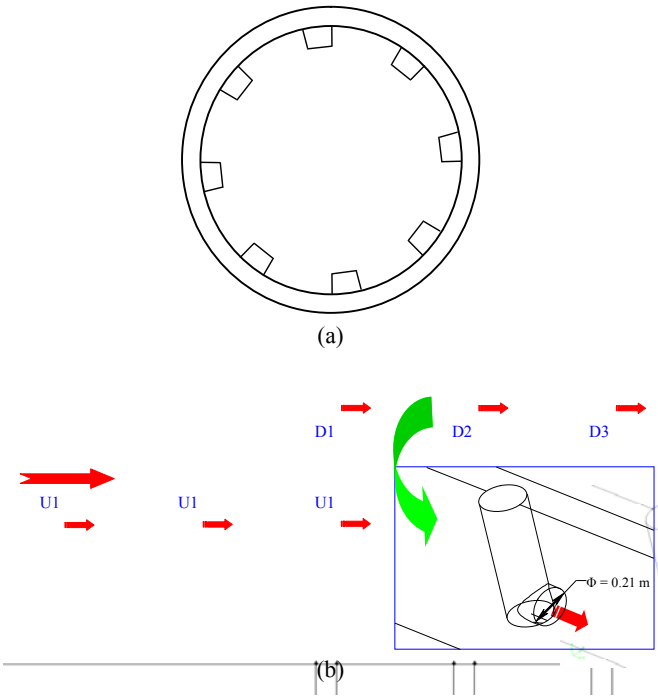

Fig. 8 (a) the cross-sectional view of the tumbler (b) tertiary air injector arrangement

Governing Equations

The conservation equations for mass, momentum and energy conservation in general form are shown below.

$$\frac{\partial \rho}{\partial t} + \nabla \bullet (\rho \vec{v}) = 0 \qquad \text{(Eq.6)}$$

$$\frac{\partial}{\partial t}(\rho \vec{v}) + \nabla \bullet (\rho \vec{v}\vec{v}) = -\nabla p + \nabla \bullet \left(\bar{\bar{\tau}}\right) + \rho \vec{g} + \vec{F} \qquad \text{(Eq.7)}$$

$$\frac{\partial}{\partial t}(\rho E) + \nabla \bullet \left(\vec{V}(\rho E + p)\right) = \nabla \bullet \left(k_{eff} \nabla T - \sum_j h_j \vec{J}_j + \left(\bar{\bar{\tau}}_{eff} \bullet \vec{v}\right)\right) + S_h \qquad \text{(Eq.8)}$$

The momentum equations are solved with the complete three-dimensional Navier-Stokes equations, so, $\bar{\bar{\tau}}$, the stress tensor is given by

$$\bar{\bar{\tau}} = \mu\left[\left(\nabla\vec{v} + \nabla\vec{v}^{T}\right) - \frac{2}{3}\nabla\bullet\vec{v}\bullet I\right] \quad \text{(Eq.9)}$$

where I is the unit tensor.

In the energy equation E is given as

$$E = h - \frac{p}{\rho} + \frac{v^2}{2} \quad \text{(Eq.10)}$$

"h" is the sensible enthalpy and for incompressible flow it is given as

$$h = \sum_j Y_j h_j + \frac{p}{\rho} \quad \text{(Eq.11)}$$

$$h_j = \int_{T_{ref}}^{T} c_{p,j} dT \quad \text{(Eq.12)}$$

T_{ref} is the reference temperture, taken as 298.15 K

S_h in the energy equation is the source term and is provided by the net enthalpy formation rates from the species transport reactions.

The flow and thermal variables are defined by the boundary conditions. The boundary conditions on the model surfaces are assigned below:

1. Velocity inlet -- All the inlets are defined as velocity inlet with a uniform velocity distribution. Velocity, temperature of the mixture, and mass fraction of all species in the mixture are assigned according to the values given below:

   a. Main inlet:

      i. Velocity inlet condition:
         1) $v_{main\ inlet}$ = 20 m/s
         2) Air volume flow rate = 2,505.12 SCFM
         3) CH_4 feed rate = 230.37 kg/hr

      ii. Temperature condition, Tmain inlet = 300 K
      iii. Mass fraction: O2 = 0.22, CH_4 = 0.043 (lean), and N_2 = 0.737 (If no other species are included, these mass fractions should add up to 1.)

   b. Tertiary air inlet:

      i. Velocity inlet condition:
         1) $v_{main\ inlet}$ = 50 m/s
         2) Air volume flow rate = 18,279.43 SCFM
      ii. Temperature condition, $T_{main\ inlet}$ = 300 K
      iii. Mass fraction:O_2 = 0.23 and N_2 = 0.77

2. Pressure outlet -- The outlet surfaces are defined as pressure outlet. The pressure, temperature, and species mass fraction of the mixture of the reverse flow are specified as follows:

   a. Gas outlet: Constant pressure outlet condition, P = 1 atm
   b. Temperature condition, T_{outlet} = 300 K
   c. Mass fraction:O_2 = 0.23 and N_2 = 0.77

3. Source layers are assigned as follows:

   a. Coke fines combustion source layer from Z = 0 to 12.19 m; Releasing rate = 0.0505 kg/m^3-s. (This is to simulate the coke fines entrainment effect and provide a carbon source for combustion.)

   b. Volatiles and coke fines source layer from Z = 12.19 to 36.58 m. (This is to simulate both the volatiles releasing and the coke fines entrainment effect as the source of combustion.):
      i. Carbon releasing rate = 0.0505 kg/m^3-s
      ii. Volatiles releasing rate = 0.1534 kg/m^3-s

   c. Heat sink layer - Energy absorption rate = 346,989.3 W/m^3. (This is to simulate the moisture evaporation absorbing energy from the gas flow.)

   d. Wall -- The outer rims of the geometry are defined as a wall boundary. The walls are treated as adiabatic (heat flux = 0) with no-slip velocity condition: u = 0, v = 0, w = 0 relatively to the wall, but the wall is rotating at 0.133 rad/s (1.27 rpm)

Computational Domain

The simulations are conducted in the following stages.

1. Thermal-flow behavior with different tertiary air **injector positions** related to the coke bed (Fig. 9 a)
2. Thermal-flow behavior with different tertiary air **injection angles** (Fig. 9 b)
3. Thermal-flow behavior with moving petrcoke bed (i.e. conjugate situation)

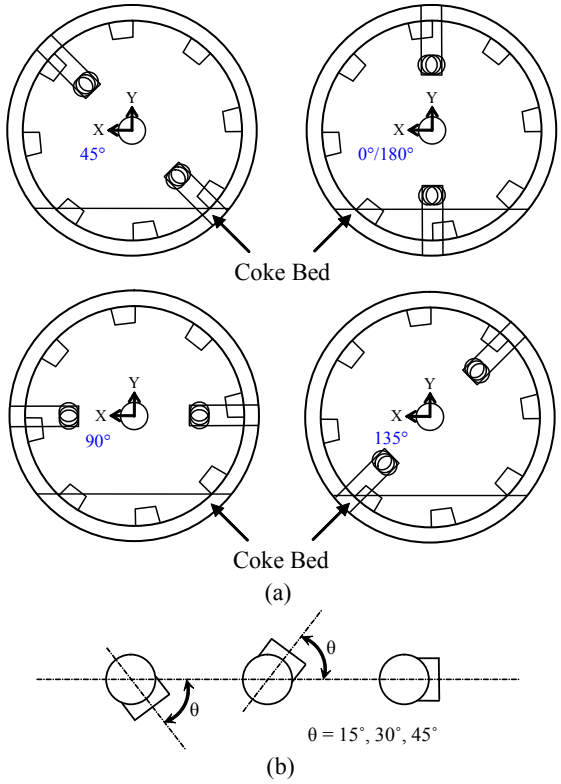

Fig. 9 (a) Relative coke bed and tertiary air inlet position (rotational angles) (b) there different tertiary air injection angles

Note: In a real situation, the coke bed tilts at an angle approximately 15°. Since the injector's location is cited relative to the coke bed, it is more convenient to show the figures without tilting the coke bed.

Turbulence Model

Turbulent flows are characterized by spectrally broad-band and randomly fluctuating velocity fields. These fluctuations advect transported quantities such as momentum, energy, and species concentration and cause the transported quantities to fluctuate as well. Since these fluctuations can be of small scale and high frequency, they are too computationally intensive to simulate directly in practical engineering calculations. Instead, the instantaneous governing

equations can be time averaged, ensemble-averaged, or otherwise manipulated to remove the small scales, resulting in a modified set of equations that are computationally less expensive to solve. However, the modified equations contain additional unknown variables, and turbulence models are needed to determine these variables in terms of known quantities.

Among many different turbulence models, this study selects the standard k - ε model due to its suitability for a wide range of wall-bounded and free-shear flows. The standard k - ε model is the simplest of turbulence two-equation model in which the solution of two separate transport equation allows the turbulent velocity and length scales to be independently determined. The k - ε model is a semi-empirical model with several constants obtained from experiments.

The standard k - ε model is a semi-empirical model based on model transport equations for the turbulence kinetic energy (k) and its dissipation rate (ε). The model transport equation for (k) is derived from the exact equation, while the model transport equation for (ε) is obtained using physical reasoning and bears little resemblance to its mathematically exact counterpart.

The turbulence kinetic energy, (k), and its rate of dissipation, (ε), are obtained from the following transport equations:

$$\frac{\partial}{\partial t}(\rho k)+\frac{\partial}{\partial x_i}(\rho k u_i)=\frac{\partial}{\partial x_j}\left[\left(\mu+\frac{\mu_t}{\sigma_k}\right)\frac{\partial k}{\partial x_j}\right]+G_k+G_b-\rho\varepsilon-Y_M+S_k \quad \text{(Eq.13)}$$

$$\frac{\partial}{\partial t}(\rho\varepsilon)+\frac{\partial}{\partial x_i}(\rho\varepsilon u_i)=\frac{\partial}{\partial x_j}\left[\left(\mu+\frac{\mu_t}{\sigma_\varepsilon}\right)\frac{\partial \varepsilon}{\partial x_j}\right] + C_{1\varepsilon}\frac{\varepsilon}{k}(G_k+C_{3\varepsilon}G_b)-C_{2\varepsilon}\rho\frac{\varepsilon^2}{k}+S_\varepsilon \quad \text{(Eq.14)}$$

In these equations, G_k represents the generation of turbulence kinetic energy due to the mean velocity gradients and the Reynolds stress, calculated as

$$G_k=-\overline{\rho u_i' u_j'}\frac{\partial u_j}{\partial x_i} \quad \text{(Eq.15)}$$

G_b represents the generation of turbulence kinetic energy due to buoyancy, calculated as

$$G_b=\beta g_i\frac{\mu_t}{Pr_t}\frac{\partial T}{\partial x_i} \quad \text{(Eq.16)}$$

where Pr_t is the turbulent Prandtl number and g_i is the component of the gravitational vector in the i-th direction. For standard k - ε model the value for Pr_t is set to be 0.85 in this study. β is the coefficient of thermal expansion and is given as

$$\beta=-\frac{1}{\rho}\left(\frac{\partial\rho}{\partial T}\right)_P \quad \text{(Eq.17)}$$

Y_M represents the contribution of the fluctuating dilatation in compressible turbulence to the overall dissipation rate, and is given as

$$Y_M=2\rho\varepsilon M_t^2 \quad \text{(Eq.18)}$$

where M_t is the turbulent Mach number, given as

$$M_t=\sqrt{\frac{k}{a^2}} \quad \text{(Eq.19)}$$

where $a=(\gamma RT)^{0.5}$ is the speed of sound.
The turbulent (or eddy) viscosity, μ_t, is computed by combining k and ε as

$$\mu_t=\rho C_\mu\frac{k^2}{\varepsilon} \quad \text{(Eq.20)}$$

$C_{1\varepsilon}$, $C_{2\varepsilon}$, C_μ, σ_k and σ_t are constants and have the following values, $C_{1\varepsilon}=1.44$, $C_{2\varepsilon}=1.92$, $C_\mu=0.09$, $\sigma_k=1.0$, and $\sigma_t=1.3$

These constant values have been determined from experiments with air and water for fundamental turbulent shear flows including homogeneous shear flows and decaying isotropic grid turbulence. They have been found to work fairly well for a wide range of wall-bounded and free-shear flows. The initial value for k and ε at the inlets and outlets are set as 1 m^2/s^2 and 1 m^2/s^3 respectively.

In general, turbulent flows are significantly affected by the presence of walls. Very close to the wall, viscous damping reduces the tangential velocity fluctuations. While kinematic blocking reduces the normal fluctuations, away from the wall, the turbulence is increased by the production of turbulence kinetic energy. In the near-wall region, the solution variables have large gradients, and the momentum and other scalar transports occur strongly. Therefore, accurate representation of the flow in the near-wall region is required for successful predictions of wall-bounded turbulent flows.

The k - ε turbulence model used in this study is primarily valid for turbulent core flows (i.e., the flow in the regions somewhat far from walls). Wall functions are used to make this turbulence model suitable for wall-bounded flows. Wall functions are a collection of semi-empirical formulas and functions that link the solution variables at the near-wall cells and the corresponding quantities on the wall. The wall functions consist of the following:

1. Laws of the wall for mean velocity and temperature and other scalars
2. Equations for near-wall turbulent quantities.

The law-of-the-wall for mean velocity gives

$$U^+=\frac{1}{\kappa}\ln(Ey^+) \quad \text{(Eq.21)}$$

where

$$U^+\equiv\frac{U_P C_\mu^{0.25}k_P^{0.5}}{\frac{\tau_w}{\rho}} \quad \text{(Eq.22)}$$

$$y^+\equiv\frac{\rho C_\mu^{0.25}k_P^{0.5}y_P}{\mu} \quad \text{(Eq.23)}$$

κ = Von Karman constant (= 0.42)
E = empirical constant (= 9.793)
U_P = mean velocity of the fluid at point P
k_P = turbulence kinetic energy at point P
y_P = distance from point P to the wall
μ = dynamic viscosity of the fluid
The logarithmic law for mean velocity is valid for y^+ > about 30 to 60
The law-of-the-wall for temperature is given

$$T^+\equiv\frac{(T_w-T_P)\rho c_P C_\mu^{0.25}k_P^{0.5}}{q''}=Pry^+ + 0.5\rho\,Pr\frac{C_\mu^{0.25}k_P^{0.5}}{q''}U_P^2 \quad \left(y^+<y_T^+\right) \quad \text{(Eq.24)}$$

$$=Pr_t\left[\frac{1}{\kappa}\ln(Ey^+)+P\right]+0.5\rho\frac{C_\mu^{0.25}k_P^{0.5}}{q''}\left[Pr_t U_P^2+(Pr-Pr_t)U_c^2\right] \quad \left(y^+>y_T^+\right) \quad \text{(Eq.25)}$$

where P is computed using the formula

$$P = 9.24\left[\left(\frac{Pr}{Pr_t}\right)^{3/4} - 1\right]\left[1 + 0.28\,e^{-0.007\,Pr/Pr_t}\right] \qquad \text{(Eq.26)}$$

k_f = thermal conductivity of the fluid
ρ = density of fluid
c_P = specific heat of fluid
q" = wall heat flux
T_P = temperature at the cell adjacent to the wall
T_w = temperature at the wall
Pr = molecular Prandtl number ($\mu c_P / k_f$)
Pr_t = turbulent Prandtl number (= 0.85 at the wall)
A = 26 (Van Driest constant)
κ = 0.4187 (Von Karman constant)
E = 9.793 (wall function constant)
U_c = mean velocity magnitude at $y^+ = y^+_T$

For k - ε turbulence model, wall adjacent cells are considered to solve the k-equation. The boundary condition for k imposed at the wall is $\partial k/\partial n = 0$, where "n" is the local coordinate normal to the wall. The production of kinetic energy, G_k, and its dissipation rate, ε, at the wall-adjacent cells, which are the source terms in k-equation, are computed on the basis of equilibrium hypothesis with the assumption that the production of k and its dissipation rate assumed to be equal in the wall-adjacent control volume. The production of k and ε is computed as

$$G_k \approx \tau_w \frac{\partial U}{\partial y} = \tau_w \frac{\tau_w}{\kappa \rho C_\mu^{0.25} k_P^{0.5} y_P} \qquad \text{(Eq.27)}$$

$$\varepsilon_P = \frac{C_\mu^{0.75} k_P^{1.5}}{\kappa y_P} \qquad \text{(Eq.28)}$$

Radiation Model

The P-1 radiation model is used to calculate the flux of the radiation at the inside walls of the rotary kiln. The P-1 radiation model is the simplest case of the more general PN radiation model that is based on the expansion of the radiation intensity I. The P-1 model requires only a little CPU demand and can easily be applied to various complicated geometries. It is suitable for applications where the optical thickness aL is large where a is the absorption coefficient and L is the length scale of the domain.

The heat sources or sinks due to radiation is calculated using the equation

$$-\nabla q_r = aG - 4aG\sigma T^4 \qquad \text{(Eq.29)}$$

where

$$q_r = -\frac{1}{3(a+\sigma_s) - C\sigma_s}\nabla G \qquad \text{(Eq.30)}$$

and q_r is the radiation heat flux, a is the absorption coefficient, σ_s is the scattering coefficient, G is the incident radiation, C is the linear-anisotropic phase function coefficient, and σ is the Stefan-Boltzmann constant.

The flux of the radiation, $q_{r,w}$, at walls caused by incident radiation G_w is given as

$$q_{r,w} = -\frac{4\pi\varepsilon_w \frac{\sigma T_w^4}{\pi} - (1-\rho_w)G_w}{2(1+\rho_w)} \qquad \text{(Eq.31)}$$

where ε_w is the emissivity and is defined as

$$\varepsilon_w = 1 - \rho_w \qquad \text{(Eq.32)}$$

and ρ_w is the wall reflectivity.

Combustion Model

Modeling for combustion ranges from nonreacting to multiple reactions with multiple species at instant rate or finite rate kinetics. In this study, combustion of methane is modeled by a single-step reaction. The mixing and transport of chemical species is modeled by solving the conservation equations describing convection, diffusion, and reaction sources for each component species. The species transport equations are solved by predicting the local mass fraction of each species, Y_i, through the solution of a convection-diffusion equation for the i-th species. The species transport equation in general form is given as:

$$\frac{\partial}{\partial t}(\rho Y_i) + \nabla \bullet (\rho \vec{v} Y_i) = -\nabla \bullet \vec{J}_i + R_i + S_i \qquad \text{(Eq.33)}$$

where R_i is the net rate of production of species i by chemical reaction. S_i is the rate of creation by addition from the dispersed phase plus any user-defined sources. $\vec{J}_i$ is the diffusion flux of species i, which arises due to concentration gradients. Mass diffusion for laminar flows is given as

$$\vec{J}_i = -\rho D_{i,m} \nabla Y_i \qquad \text{(Eq.34)}$$

For turbulent flows, mass diffusion flux is given as

$$\vec{J}_i = -\left(\rho D_{i,m} + \frac{\mu_t}{Sc_t}\right)\nabla Y_i \qquad \text{(Eq.35)}$$

where Sc_t is the turbulent Schmidt number given as $\mu_t/\rho D_t$, where μ_t is the turbulent viscosity and D_t is the turbulent diffusivity.

In this study, the reaction rate that appears as source term in (Eq.33) is given by the turbulence-chemistry interaction model called the eddy-dissipation model. The overall rate of reaction for most fast burning fuels is controlled by turbulent mixing. The net rate of production of species i due to reaction r, $R_{i,r}$, is given by the smaller of the two given expressions below:

$$R_{i.r} = \nu'_{i,r} M_{w,i} A \rho \frac{\varepsilon}{\kappa} \min_R \left(\frac{Y_R}{\nu'_{R,r} M_{w,R}}\right) \qquad \text{(Eq.36)}$$

$$R_{i.r} = \nu'_{i,r} M_{w,i} AB \rho \frac{\varepsilon}{\kappa} \frac{\sum_P Y_P}{\sum_j^N \nu''_{j,r} M_{w,j}} \qquad \text{(Eq.37)}$$

Where Y_P is the mass fraction of any product species, P
Y_R is the mass fraction of a particular reactant, R
A is an empirical constant equal to 4.0
B is an empirical constant equal to 0.5
$\nu'_{i,r}$ is the stoichiometric coefficient for reactant i in reaction r
$\nu''_{j,r}$ is the stoichiometric coefficient for product j in reaction r

In the above equation (Eq.36) and (Eq.37), the chemical reaction rate is governed by the large-eddy mixing time scale, κ/ε, and an ignition source is not required. This is based on the assumption that the chemical reaction is much faster than the turbulence mixing time scale, so the actual chemical reaction is not important.

In this study, methane (CH_4) is used as fuel, the volatile matters from the petcoke is assumed to be $CH_{3.086}O_{0.131}$ with medium heating value, and carbon (C) is used for coke combustion. The complete global stoichiometric combustion equations are given below:

$$CH_4 + 2O_2 \rightarrow CO_2 + 2H_2O \qquad \text{(Eq.38)}$$

$$CH_{3.086}O_{0.131} + 1.706O_2 \rightarrow CO_2 + 1.543H_2O \qquad \text{(Eq.39)}$$

$$C + O_2 \rightarrow CO_2 \qquad \text{(Eq.40)}$$

COMPUTATIONAL METHOD

The CFD Code Background

The commercial computational fluid dynamics (CFD) code, FLUENT, is used in this study. The momentum, energy, turbulence and species equations are discretized using the finite volume second order upwind scheme. FLUENT offers two different solvers: segregated and coupled. Segregated solver only has implicit formulation while coupled solver has implicit and explicit formulations. Segregated method solves the governing equations sequentially. On the contrary, coupled method solves the governing equations simultaneously. In this study, segregated solver is employed to solve the governing equations of the conservation of mass, momentum, energy, turbulence and the species transports. The implicit pressure-correction scheme, SIMPLE algorithm [7], is used to couple the pressure and velocity. Converged results are obtained after the specified residuals are met.

Computational Grid

The computational geometry is constructed and meshed in GAMBIT. Three-dimensional tetrahedral mesh is used for meshing the entire rotary kiln. Figure 10 illustrates the model geometry with computational grids used in the baseline case study. A total of 1,331,654 cells are employed. The computational domain is a long and slender cylinder; the length-diameter ratio is 200:9. To properly mesh the geometry and avoid grid aspect ratio problem, this domain is divided into nine sub domains as shown in Figs. 5, 6, and 7. In the diametric direction, the kiln is separated into three horizontal zones based on the property of the media as: coke bed, coke-fines/volatiles/moisture source layer, and the gas zone. In the axial direction (z-direction) from the feed end to the discharge end and based on the function of kiln, the kiln is separated into three sections: heat-up, calcining, and calcined zones. The mesh number of each sub domain is shown in Table 1.

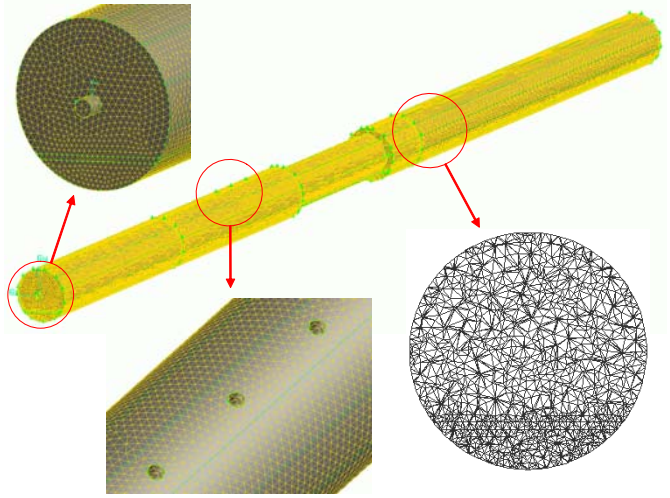

Fig. 10 Meshed geometry for the rotary calcining kiln

Table 1 Mesh numbers in the nine sub-domains

Axial Sections / Horizontal Zones	Calcined Coke Zone	Calcining Zone	Heat-up Zone
Gas Zone	251,621	282,985	356,819
Source Layer	22,036	38,173	43,353
Coke Bed	77,997	101,014	157,656

The heat-up coke bed (157,656 cells) is connected to calcining coke bed (101,014 cells) and then connected to the calcined coke bed (77,997 cells). On top of the coke bed, there is a special function layer. This layer is also separated into three portions from the feed end to the discharge end. They are heat sink layer (43,353 cells) connecting with the volatiles/coke-fines source layer (38,173 cells) and then connected to the coke fines combustion source layer (22,036 cells). The gas zone is formed by three zones, heat-up zone (356,819 cells), calcining zone (282,985 cells), and calcined zone (251,621 cells) respectively. All zones are meshed with tetrahedral mesh elements to avoid potential large aspect ratio problem, which is often seen in long and slender geometry meshed with hexahedral mesh elements. Along the cylinder wall, extra lines are created to achieve better mesh quality. The model is then exported to FLUENT after being meshed.

Numerical Procedure

The segregated method solves the governing equations sequentially with following steps:

1. Fluid properties are first updated based on the current solution or the initial conditions.
2. Momentum equations are solved with the current values of pressure and face mass fluxes to update the velocity field.
3. Equation for the pressure correction is calculated from the continuity equation and the linearized momentum equations since the velocity field obtained from step 2 may not satisfy the continuity equation.
4. The pressure correction equation obtained from step 3 is solved to acquire necessary corrections for the pressure, velocity field, and face mass fluxes such that the continuity equation is satisfied.
5. The transport equations for scalars such as turbulence, and energy are solved using the updated values of the other variables and energy source or sink term from reactions in step 6.
6. The reactions are solved with the input of the stochiometeric coefficients and adoption of the eddy dissipation model for reaction rate. Species source and energy source terms are generated for step 7 in this loop or step 5 in next loop.
7. The species transport equations are solved with the velocity filed, species concentration, and the species source term obtained from step 6.
8. The equation is checked for convergence.

These steps are repeated until the convergence criteria are met. Figure 11 shows the flow chart of the segregated method proceeding steps.

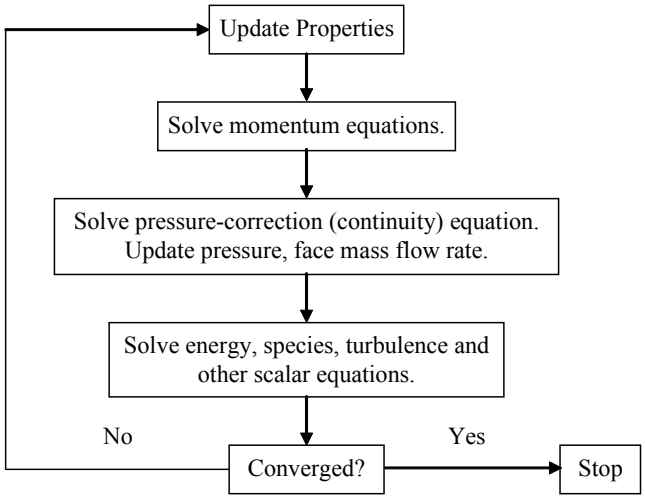

Fig. 11 Flow chart for segregated solver

The species transport model with volumetric reaction and the eddy-dissipation model are chosen to simulate the chemical reactions.

The chemical reaction rates are assumed to be faster than the mixing rates and are controlled by the turbulence time scale.

In this study, methane-air, volatile-air, and coke (carbon)-air combustions are simulated. The mixture consists of seven species (C, O_2, CH_4, mv_vol, CO_2, H_2O, and N_2). All the species in the mixture are defined as fluid species and are assumed to mix at the molecular level. The property values in the gas vary with temperature and pressure. The densities of the species obey incompressible ideal gas law, and the specific heat of the species follows the mixing law.

For the baseline case, the solution convergence is obtained by monitoring the residuals of the continuity, momentum, energy, turbulence and species equations separately: Continuity (mass conservation) < 2×10^{-3}, X-velocity < 9×10^{-5}, Y-velocity < 8×10^{-5}, Z-velocity < 2×10^{-5}, Energy < 5×10^{-5}, k (turbulence energy) < 3×10^{-4}, ε (turbulence dissipation) < 2×10^{-3}, Volatiles < 3×10^{-4}, O_2 < 3×10^{-4}, CO_2 < 6×10^{-5}, H_2O < 6×10^{-5}, C < 3×10^{-4}, CH_4 < 5×10^{-3}, and P-1 < 4×10^{-5}.

A typical physical iteration time of 5000 iterations for baseline case using 4 × Pentium 4 3.2GHz computers parallel processing requires approximate 20 hours. A cluster of 8 personal computers is used for most of the computations..

Grid Sensitivity Study

Due to the limitation of the computer power with eight desktop personal computers in parallel processing, the results have not reached grid independency. Instead, a grid sensitivity study is carried out by comparing the change of results from two different mesh sizes. The baseline case has a higher number of cells (1,331,654 cells) and the other lower mesh number case has 384,111 cells. Figure 12 shows the variation of gas zone centerline static temperature of these two cases. In the important calcining and calcined coke zones, the difference of centerline temperatures of two mesh sizes is within 50 to 200 K (3 to 12%). In the heat-up zone, which is not critical for the calcining process, the temperature difference is less than 50 K (3%). Based on this grid-sensitivity study, it is felt that the temperature differences will reduce when the mesh number are more than 1.4 million. For the purpose of current study, 10 % of computational uncertainty is acceptable.

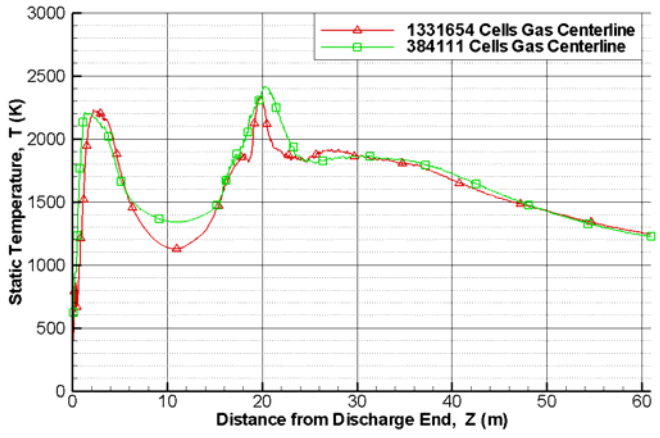

Fig. 12 Gas centerline static temperature for various cell numbers

Case Settings

Total thirteen 3-D cases and six 2-D cases are conducted. For reference of comparison, the normal (reference) operating conditions are recapped here:

- Natural gas supplying rate = 0.0640 kg/s
- Petcoke feed rate = 9.3 kg/s
- Petcoke combustion rate = 0.3456 kg/s
- Volatiles source rate = 0.6994 kg/s
- Heat sink for latent heat absorption during moisture evaporation = 346,989.3 W/m^3
- Main air inlet injection velocity and flow rate = 20 m/s, 2,504.49 SCFM
- Tertiary air inlet injection velocity and total flow rate = 50 m/s, 18,279.26 SCFM
- Adiabatic wall condition
- Kiln wall rotational velocity = 0.133 rad/s (1.27 rpm)
- Coke bed sliding velocity = 0.01 m/s
- Resident time = 1.69 hr

The results will be analyzed and discussed with the following different operating conditions:

1. Various rotational angles (Cases 5, 6, 9, 10, and 11)
2. Various tertiary air injection angles (Cases 6, 7, and 8)
3. Discharge end flow control (Cases 1, 2, and 3)
4. Discharge end flow extraction and return (Cases 5 and 13)
5. Various coke bed devolatilization conditions (Cases 5, 6, and 12)
6. Various coke bed properties (2-D Cases A, B, C, D, E, and F)

Due to the complexity of the results, only the results of various rotational angles and tertiary air injection angles will be presented in part 2 of this paper. Other results will be presented in a future paper. The corresponding 3-D case numbers, simulation conditions, and number of cells are listed in Table 2. The locations and labeling of the tertiary air injectors are shown in Fig. 13.

Table 2 3-D case number and descriptions (major variations are noted in bold font)

3D Case Number	Case Descriptions	Mesh Numbers
Case 1	0 degree tertiary inlet position, 15 degree injection angle, with coke bed, normal operation condition **(Baseline)**	1,331,654
Case 2	0 degree tertiary inlet position, 15 degree injection angle, with coke bed, normal operation condition with **10kPa suction at main inlet, and no natural gas**	1,331,654
Case 3	0 degree tertiary inlet position, 15 degree injection angle, with coke bed, normal operation condition **with 10kPa suction at main inlet and 2 upstream tertiary air injections,** and no natural gas	1,331,452
Case 4	0 degree tertiary inlet position, 15 degree injection angle, **no coke bed**, normal operation condition	751,226
Case 5	0 degree tertiary inlet position, 15 degree injection angle, no coke bed, normal operation condition **without coke fines combustion**	763,538
Case 6	**45 degree** tertiary inlet position, **15 degree injection angle,** no coke bed, normal operation condition without coke fines combustion	762,687
Case 7	45 degree tertiary inlet position, **30 degree injection angl**e, no coke bed, normal operation condition without coke fines combustion	764,546
Case 8	45 degree tertiary inlet position, **45 degree injection angl**e, no coke bed, normal operation condition without coke fines combustion	763,040
Case 9	**90 degree tertiary inlet position**, **15 degree injection angle,** no coke bed, normal operation condition without coke fines combustion	760,579
Case 10	**135 degree tertiary inlet position**, 15 degree injection angle, no coke bed, normal operation condition without coke fines combustion	764,451
Case 11	**180 degree tertiary inlet positio**n, 15 degree injection angle, no coke bed, normal operation condition without coke fines combustion	763,579
Case 12	0 degree tertiary inlet position, 15 degree injection angle, no coke bed, normal operation condition without coke fines combustion, and **shortened devolatile zone**	747,420
Case 13	0 degree tertiary inlet position, 15 degree injection angle, no coke bed, without coke fines combustion**,** no natural gas, 10kPa suction at main inlet, and **extracted hot combustion gas returned at Z = 35.052 m**	763,505

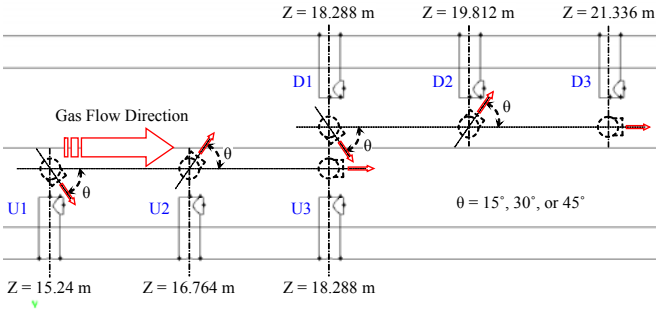

Figure 13 Tertiary air injector locations and labeling

SUMMARY

The basic petroleum coke calcining process is reviewed. The comprehensive CFD models are developed to simulate the calcining process inside a rotary calcining kiln.

ACKNOWLEDGEMENT

This study was jointly supported by Rain CII Carbon, LLC and the Louisiana Board of Regents' Industrial Ties Research Subprogram.

REFERENCES

[1] Bagdoyan, E. A., and Gootzait, E., "Refiners Calcine Coke," Hydrocarbon Processing, September 1985, pp.85-90.

[2] Ellis, P. J., and Paul, C. A., "Tutorial: Petroleum Coke Calcining and Uses of Calcined Petroleum Coke," AIChE 2000 Spring National Meeting, Third International Conference on Refining Processes, Session T9005, March 2000.

[3] Zhao, L. and Wang, T., "Investigation of Potential Benefits of Using Bricks of High Thermal Capacity and Conductivity in a Rotating Calcining Kiln," ASME paper HT08-56455, presented at the ASME 2008 Summer National Heat Transfer Conference, August 10-14, 2008, Jacksonville, FL, USA

[4] Brooks, D. G., "Mathematical Simulation of a Rotary Coke Calciner," Light Metals, 1989, pp. 461-469.

[5] Kaiser Aluminum, "The Use of Refractory Tumblers in Coke Calcination," Kaiser Aluminum brochure, circa 1983.

[6] Merrill, Jr., and Lavaun, S., "Particulate Emissions from A M-W Rotary Hearth Calciner," Light Metals, 1978.

[7] Patankar, S.V., "Numerical Heat Transfer and Fluid Flow," McGraw-Hill Inc., Hemisphere, 1980.

[8] Allred, V. D., "Rotary Hearth Calcining of Petroleum Coke," Light Metals, 1971, pp. 313-329.

[9] Anderson, J. D. Jr, "Computational Fluid Dynamics, the basics with application," McGraw-Hill Inc., 1995.

[10] Burmeister, L. C., "Convective Heat Transfer," John Wiley & Sons Inc., 1983.

[11] CII Carbon L.L.C., "Canadian Rotary Coke Calciner Modeling," 2004.

[12] FLUENT 6.1 User's Guide, February 2003.

[13] Incropera, F. P., and DeWitt, D. P., "Introduction to Heat Transfer," 4th Edition, John Wiley & Sons Inc., 1996.

[14] Munson, Young, and Okiishi, "Fundamentals of Fluid Mechanics," 3rd Edition, John Wiley & Sons Inc., 1998.

[15] Siegel, R., and Howell, J. R., "Thermal Radiation Heat Transfer," Hemisphere Publishing Corporation, Washington D.C., 1992.

[16] Tennekes, H., and Lumley, J. L., "A First Course in Turbulence," The Massachusetts Institute of Technology, 1972.

[17] Thomas, L. C., "Heat Transfer," 2nd edition, Capstone Publishing Corporation., 2000.

[18] Turns, Stephen R., "An Introduction to Combustion," 2nd Edition, McGraw-Hill Inc., 2000.

[19] Van Wylen, G. J., Sonntag, R. E., "Fundamentals of Classical Thermodynamics," 3rd Edition, John Wiley & Sons Inc., 1986.

[20] White, Frank, "Viscous Flow," 2nd edition, McGraw-Hill Inc., 1991.